1-1

高温衝撃風洞の駆動気体汚染に関する数値計算

ランディ チュー　　伊藤勝宏
航技研 角田研究センター

A Computational Study of Driver Gas Contamination in a High Enthalpy Shock Tunnel

by

Randy S. M. CHUE and Katsuhiro ITOH
National Aerospace Laboratory, Kakuda Research Center
1 Kimigaya, Koganesawa, Kakuda
Miyagi, JAPAN 981-15

Abstract

A computational study has been carried out to examine driver gas contamination in a high-enthalpy reflected shock tunnel. The investigation focused on the nonsteady events as the reflected shock interacts with the wall boundary layer and the contact interface and their contribution to driver gas contamination. Both tailored and off-tailored tunnel operating conditions and the effects of a choked nozzle are discussed in the present paper.

1. Introduction

In reflected-shock tunnel facilities, the reflection of the incident shock at the end of the shock tunnel generates a reservoir of high enthalpy gas which, upon flowing through a nozzle, provides a source of high Mach number flow that can be utilized for aerodyamic testing. The ideal testing time of the facility is governed by the duration for the test gas slug to be exhausted through the nozzle. If, however, the driver gas arrives prematurely at the nozzle, the testing time of the facility would be decreased. The contamination of the test gas by driver gas is an important problem in shock tunnel testing and particularly in high enthalpy impulse facilities where the the useful test time would severely be limited.

The interaction of the reflected shock with viscous boundary layers has been recognized as one of the major candidates to cause driver gas contamination. The theoretical treatment first developed by Mark[1] has established the framework for understanding the resulting bifurcated shock structure and the transport of boundary layer fluid by wall jetting towards the end of the shock tube. Based on this mechanism, analytical models have been developed to estimate the premature arrival of the driver gas at the shock tube end-plate (e.g., Davies & Wilson[2], Stalker & Crane[3]). More recently numerical simulations have provided more detailed information about the contamination process (e.g. Wilson et al.[4]), which has become a great concern in the current interest in high enthalpy impulse facilities. Wilson examined the bifurcated shock structure and the transport of driver gas along the wall to the end-plate for an over-tailored case with laminar boundary layer.

However, the mechanism that is responsible for the premature arrival of driver gas remains unclear and therefore it is still difficult to predict driver gas contamination in reflected-shock tunnels. Furthermore, many experimental works done to understand the phenomena are carried out under relatively low incident shock Mach numbers (of less than 6) and are therefore not sufficient for high enthalpy studies. Also, because the main interest has been the phenomenon of reflected shock/boundary layer interaction itself, most of the experimental and computational works tended to be done for strongly over-tailored conditions where the interaction is more significant and easily observable. The tailored operating condition, which is of greater relevance to high enthalpy testing, has not been clearly examined.

Stalker and his colleagues have been carrying out experimental measurements and analytical predictions of driver gas contamination based on the interaction of reflected shock and wall boundary layers in their high-enthalpy free-piston shock tunnel and have found that the tunnel testing time was signifi-

cantly reduced at high enthalpies (see for example, Skinner[5]). The experiments and analyses have been carried out for fixed driver condition with variable shock tube initial conditions. Thus far, their analytical predictions of the arrival of driver gas at the test section has not shown reasonable agreement with the experimental results. Moreover, the experimental detection of driver gas remains a difficult problem and it is not easy to vary the tunnel operating conditions in actual experiments. Computational study is thus expected to be an important tool for examining driver gas contamination.

The objective of the present work is twofold—to analyze computationally the reflected shock/boundary layer interaction in order to determine its role in causing driver gas contamination and the lost of testing time, and to conduct numerical experiments to evaluate the influence of different tunnel operating conditions on driver gas leakage.

2. The Computational Model

Time-dependent viscous calculations were carried out for a reflected-shock tunnel with circular cross-section. The shock tube investigated is assumed to have dimensions: internal diameter 30 mm, length 4 m, shock-tube-to-driver-tube area ratio 0.09. The computational domain covered only the region near the end of the shock tube with the upstream inflow condition and the tube-wall temperature assumed to be fixed. Because the emphasis is on the events after the incident shock has reflected from the end-plate of the shock tube, the initial condition of the computation was taken at the moment just before shock reflection, with the initial flow field behind the shock estimated from the turbulent boundary layer theory of Mirels[6].

The present study focuses on high shock Mach numbers ($M_s \simeq 10$) typically encountered in high enthalpy impulse facilities. The driver and driven gases are helium and air, respectively, which are assumed to be perfect gases. The driver gas has specific heat ratio of 5/3 and molecular mass of 4.003 kg/kmol. The test gas is assumed to be high temperature air having specific heat ratio of 1.25, molecular mass of 25.9 kg/kmol. The viscous boundary layer along the tube wall is assumed to be turbulent and the Baldwin-Lomax[7] algebraic eddy viscosity model is used in the present preliminary analysis. To single out the effect of reflected shock/boundary layer interaction, the contact region between the driver and driven gases is initially assumed to be a plane discontinuous surface and no attempt is made to consider the effects of non-ideal diaphragm rupture and mixing.

The computational code used in the analysis is developed by Takahashi et al.[8] using a second order KRC scheme, which is a pointwise nonoscillatory shock capturing method developed by Itoh et al.[9] Time integration was done using the second order Runge-Kutta method. The computational mesh covers 26 cm of the end portion of the shock tube with a 433×121 grid with clustering in the boundary layer and the end-plate regions. A more detailed account of the numerical method used and its validation can be found in Takahashi et al.[8]

3. Results and Discussions

Two sets of computations have been carried out—one for a closed-end shock tube and another for a shock tunnel with a choked nozzle. The shock Mach number (M_s) is fixed at 10 with initial shock tube pressure (p_1) at 10 kPa. The total enthalpy behind the reflected shock is 13 MJ/kg.

3.1 Wall Jetting

Figure 1 presents the sequence of contour plots of temperature and driver gas mass fraction as the reflected shock interacts with the turbulent boundary layer for times up to 100 μsec after shock reflection at the end-plate. In this calculation, the "tailored" interface condition, where the ratio of transmitted shock pressure to the reflected shock pressure (p_7/p_5) equals 1.0, is enforced. Particular attention is directed towards the bifurcated shock structure produced as the reflected shock propagates into the boundary layer flow. The formation of the bifurcated shock and the resulting mechanism of wall jetting of the "cold" boundary layer fluid towards the end-plate which generates a vortex at the corner region of the end-plate is clearly illustrated in Fig. 1a. The distortion of the contact surface and the leakage of driver gas into the test gas through the bifurcated shock foot can be seen in Fig. 1b. The interaction immediately results in a stream of driver gas, near the edge of the boundary layer and the triple point of the bifurcated shock, being driven towards the wall boundary layer and is then partially transported towards the end-plate (at 50 μsec). This phenomenon agrees well with the previous analytical model proposed (Mark[1], Davies & Wilson[2]). However, the vortical structure generated at the contact surface has a counter-clockwise direction which serves to retard further transport of driver gas towards the end-plate. Moreover, the bifurcated shock structure weakens drastically as the reflected shock transmits through the contact surface and wall jetting is less apparent as the shock propagates into the driver gas region. It is also noted that the contact surface shape remains rather

planar as would be predicted by inviscid theory, except near the boundary layer region. The driver gas transported by wall jetting arrives at the end-plate at about 95 μsec after shock reflection.

3.2 Off-tailored Interface Conditions

The effects of off-tailored tunnel conditions are compared in Fig. 2. Figures 2a and 2c show the temperature and driver gas mass fraction distributions at 100 μsec for off-tailored conditions while keeping the primary shock Mach number to be 10. The values of p_7/p_5 are respectively 0.8 and 1.1 for the under- and over-tailored conditions. The tailored case is redisplayed in Fig. 2b for comparison. The effect of wall jetting is most severe for the over-tailored condition as driver gas arrives at the end-plate the earliest, but the overall shape of the contact surface remains largely undistorted. On the other hand, the effect of reflected shock/boundary layer interaction appears to be least severe for the under-tailored case where wall jetting is too weak to transport the driver gas towards the end-plate. However, the vortex-generated flow strongly distorts the contact surface near the center-line and builds up a large protruded region of driver gas that flows towards the end-plate.

The present results therefore indicate that reflected shock/boundary layer interaction does not necessarily play the major role in the driver gas contamination process as the driver gas may be transported towards the end-plate by other means. The nature of the vortex dynamics produced also appeared not to favor driver gas leakage by purely the mechanism of wall jetting alone. This points out the need to examine other mechanisms, such as instabilities and mixing in the contact region, in causing driver gas contamination in experiments where the lost of testing time had been observed to be more severe.

Besides the contamination by "cold" wall fluid and driver gas, Fig. 3 shows that the pressure at the center of the shock-tube end plate becomes quite nonsteady with a large pressure peak occurring near 80 μsec for both the tailored and off-tailored cases. The quality of the freestream flow would then be affected if the gas is allowed to discharge through a nozzle at the end of the shock tunnel.

3.3 Effect of Nozzle Flow

As an initial effort to include the effect of nozzle flow at the end of the shock tube, a calculation is performed assuming the nozzle to be an effective "sink" with choked flow. The nozzle throat diameter is taken to be 10 mm. The exhaust flow takes effect as soon as the shock has arrived at the end-plate and is assumed to be choked based on the condition in the center-line immediately upstream of the end-plate. Although the present analysis may be overly crude for describing the actual shock/nozzle flow interaction, it should provide a qualitative picture of how the driver gas may exhaust into the nozzle. Figure 4 shows the sequence of contour plots of temperature and driver gas mass fraction for the tailored condition as the driver gas is transported towards the nozzle. The early events of reflected shock/boundary layer interaction is quite similar to the case without the nozzle, although the vortex at the corner of the end-plate appears to be larger with nozzle flow (c.f. Fig. 1). From 80 μsec, the volume of driver gas leakage at the end-plate appears to be entrained into a vortex closed to the end-plate, with a stagnation point dividing the vortex and the exhaust flow slightly upstream of the nozzle on the center-line. Because of this, only part of leakage gas is exhausted into the nozzle with the rest being recirculated in the shock tube (100 μsec). The time of arrival of driver gas at the nozzle is at 90 μsec and is not significantly different from the closed-end case. A set of off-tailored conditions has also been recalculated with the nozzle flow, and the results are again quite close to those for the closed-end conditions presented in Fig. 2.

3.4 Loss of Test Time

The arrival time of the driver gas at the end plate is summarized in Table 1 for the tailored condition. Also included in the table are the values calculated using the analytical approximation of Davis & Wilson[2], based on the mechanism of wall jetting, and the "ideal" drainage time for reference. The drainage time is the time required to drain the test gas with consideration of mass loss due to boundary layer effects prior to shock reflection. The approximation of Davies obtained a value on the conversative side and can be a useful tool for predicting test time in actual tunnel operations if the effect of wall jetting is dominant. However, as wall jetting may not always be the cause of driver-gas contamination, as illustrated earlier in the under-tailored condition, the formulation may not always be adequate. In any case, the premature arrival of the driver gas can significantly reduce test time. For the shock tunnel considered in the present study, the arrival time of driver gas is less than 50% of the drainage time.

4. Concluding Remarks

The interaction of reflected shock with a turbulent boundary layer has been analyzed numerically to assess its contribution to driver gas contamina-

tion. The results illustrated that the contamination of test gas can be manifested in at least two ways—the transport of low-temperature boundary layer fluid as well as driver gas leakage. While the results demonstrated that wall jetting is an important mechanism to cause contamination of the test gas, it may not necessarily be the dominating one. In particular, the mechanism for contamination is quite dependent on the tunnel operating condition with under-tailoring appeared to be affected more by the distortion of the contact surface rather than by wall jetting. It is thus necessary to consider other mechanisms, such as contact surface instabilities and mixing subsequent to diaphragm rupture, before a more precise understanding of driver gas contamination can be achieved.

Acknowledgement

Special thanks are due to M. Takahashi for his help and discussions, and to G. Eitelberg of DLR-Göttingen for suggesting the calculation with nozzle flow. R.S.M. Chue is supported by the STA Fellowship program of Japan.

References

[1]Mark, H., "The Interaction of a Reflected Shock Wave with the Boundary Layer in a Shock Tube," NACA TM 1418, 1958.

[2]Davies, L. and Wilson, J. L., "Influence of Reflected Shock and Boundary-Layer Interaction on Shock-Tube Flows," *The Phys. of Fluids Supplement I*, pp. I-37–I-43, 1969.

[3]Stalker, R. J. and Crane, K. C. A., "Driver Gas Contamination in a High-Enthalpy Reflected Shock Tunnel," *AIAA Journal*, Vol. 16, pp. 277-279, 1978.

[4]Wilson, G. J., Sharma, S. P., and Gillespie, W. D., "Time-Dependent Simulations of Reflected-Shock/Boundary Layer Interaction," AIAA Paper 93-0480, 1993.

[5]Skinner, K. A., "Mass Spectrometry in Shock Tunnel Experiments of Hypersonic Combustion," Ph.D thesis, Department of Mechanical Engineering, The University of Queensland, March 1994.

[6]Mirels, H., "Shock Tube Test Time Limitation Due to Turbulent-Wall Boundary Layer," *AIAA Journal*, Vol. 2, pp. 38-54, 1964.

[7]Baldwin, B. S., and Lomax, H., "Thin Layer Approximation and Algebraic Model for Separated Turbulent Flows," AIAA Paper no. 78-257, 1978.

[8]Takahashi, M., Itoh, K., Tani, K., and Tanno, H., "Numerical Analysis of the Driver Gas Contamination in a Reflected Shock Tunnel," In: *Proc. of Symp. on SHOCK WAVES, JAPAN '94* (in Japanese), pp 211-214, 1994.

[9]Itoh, K., Takahashi, M., and Hiraiwa, T., "Pointwise Non-Oscillatory Shock Capturing Scheme," In: *Proc. of 6th Symp. on Computational Fluid Dynamics* (in Japanese), pp 535-538, 1992.

Table 1: Time of arrival of driver gas at the end wall.

	Time after shock reflection (μsec)
Closed-off end wall	95
With nozzle	90
Analytical approx. by Davies	62
"Ideal" drainage time [a]	226

[a] $t_{drainage} = \frac{4M}{A^*}\frac{1}{\rho_5 a_5}\left(\frac{\gamma+1}{2}\right)^{\frac{\gamma+1}{2(\gamma-1)}}$, M = mass of test slug, a = sound speed, and A^* = nozzle throat area. Subscript 5 denotes the condition behind the reflected shock.

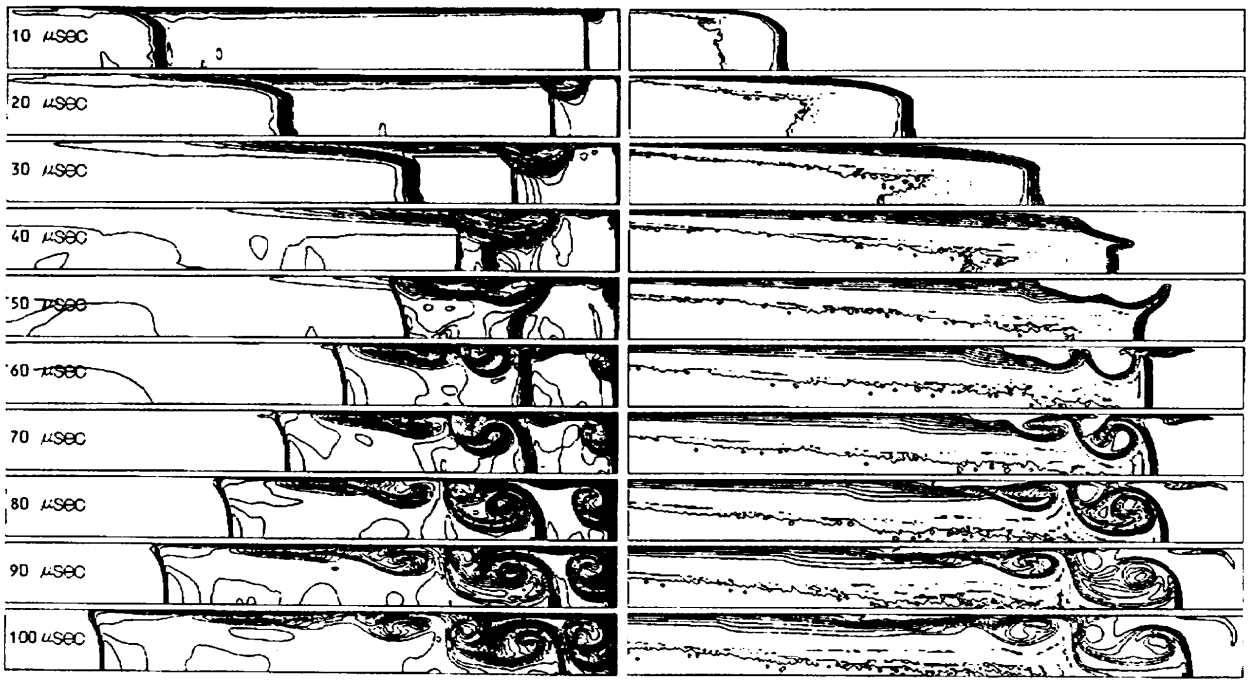

(a) Temperature (b) Driver gas mass fraction

Figure 1: Temperature and driver-gas contours after shock reflection.

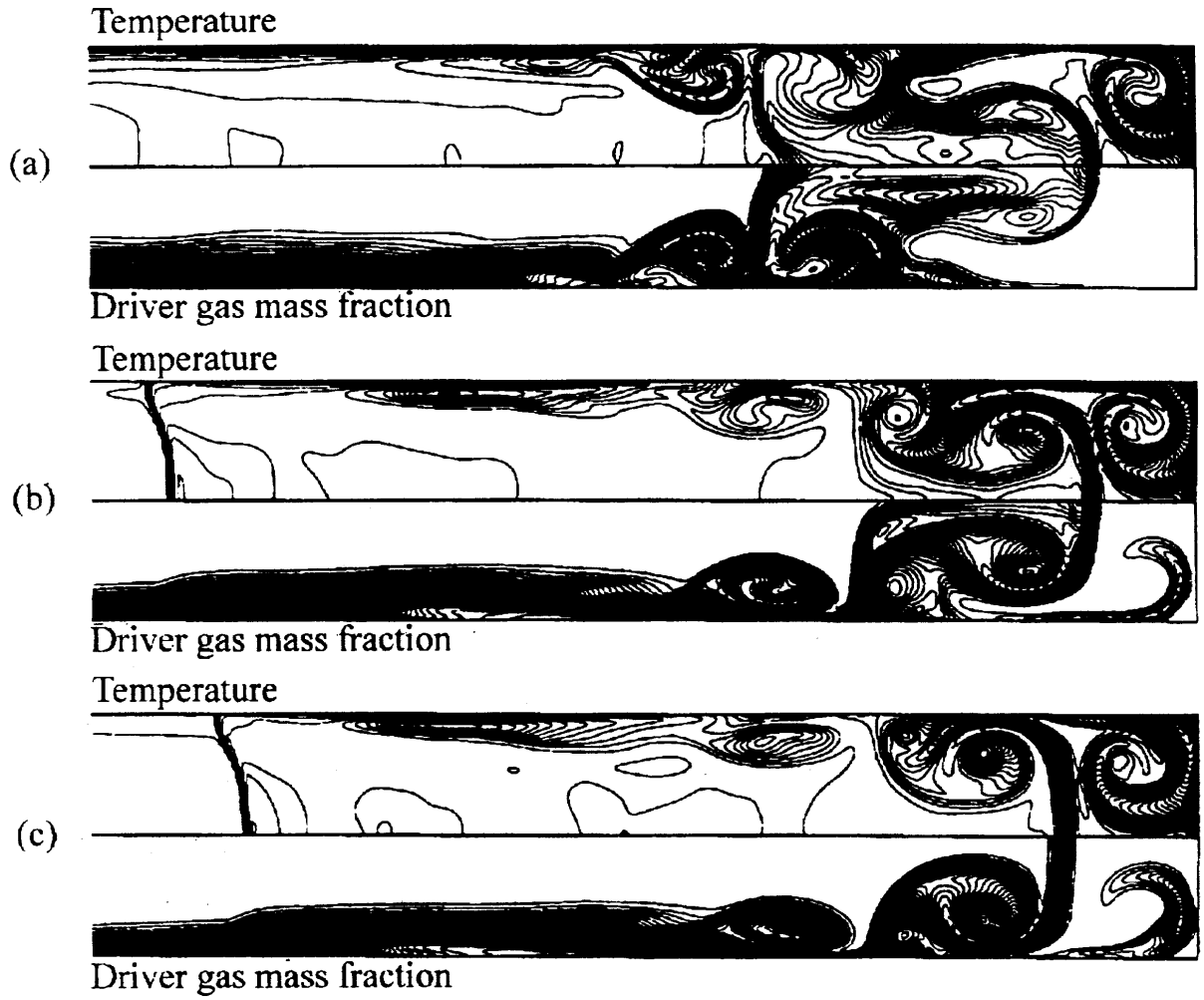

Figure 2: Effect of tunnel operating condition on driver gas contamination at $t = 100$ μsec: (a) Under-tailored. (b) tailored. and (c) over-tailored condition.

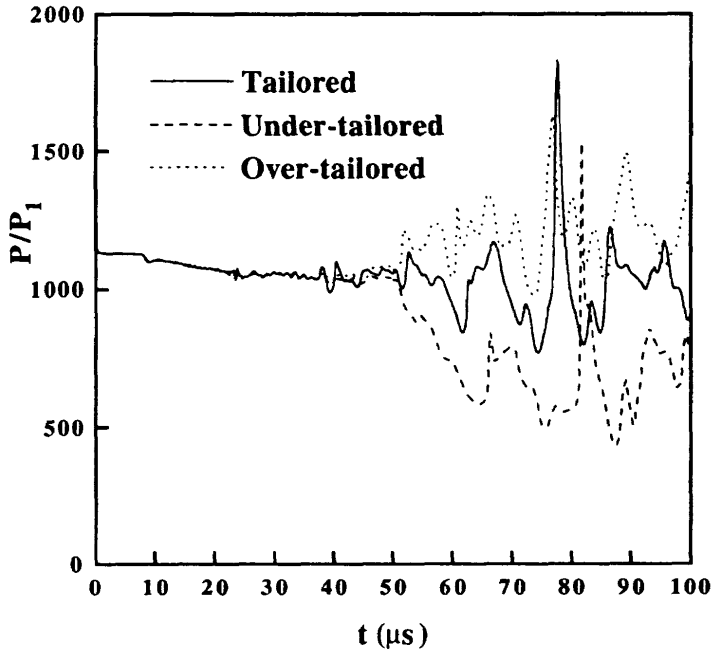

Figure 3: Pressure (p/p_1) history at the center of the shock-tube end plate.

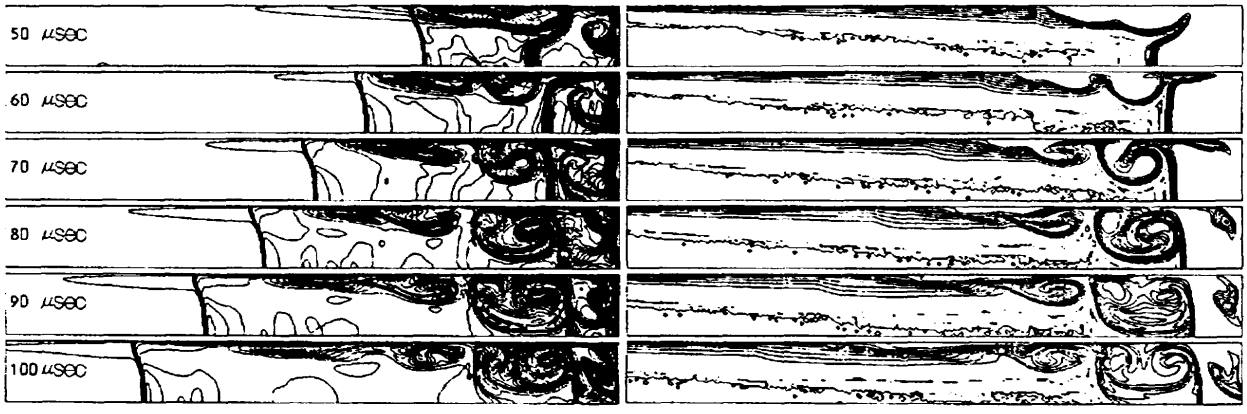

(a) Temperature (b) Driver gas mass fraction

Figure 4: Effect of nozzle flow on driver gas transport. $M_s = 10$, tailored interface condition.

1-2

HIGH ENTHALPY FLOW COMPUTATION AND EXPERIMENT AROUND THE SIMPLE BODIES

A.HANAMITSU T.KISHIMOTO
Kawasaki Heavy Industries, Ltd.

and

H.BITO
National Space Development Agency of Japan

Abstract

High enthalpy shock tunnel test was performed at HEG (High Enthalpy Shock Tunnel in Göttingen) to examine the real gas effect on shock interference heating. Heat transfer distributions were measured along the sphere model and the leading edge of simple wing-body model, whose sweep-back angle on the starboad side is 55° and on the port side is 60° . Flow visualization was also made for simple wing-body model by LIF (Laser Induced Fluorescence) method. CFD analysis has been performed about the heat transfer distribution along the sphere model both in the conditions of frozen flow and equilibrium air flow. Good agreement with experiment was achived in the condition of equilibrium air flow.

This test program was performed under contract with National Space Depelopment Agency of Japan, NASDA, and is a part of wind tunnel test programs for HOPE (H-II Orbiting Plane) development.

Introduction

HOPE developement program has been proceeding by NAL and NASDA. Aerothermodynamic design of HOPE is one of the main problem in the design of HOPE config-uration. It is much more severe than that of Space Shuttle Orbiter, because the scale is about one third of Space Shuttle Orbiter. It is required to accurately predict the aerothermodynamic environment during reentry, especially in high temperature hypersonic flight regime, where maximum heat transfer occurs.

To measure heat transfer in high temperature hypersonic flight regime, there are two flight experiment program in Japan. One was the Orbital Reentry Experiment (OREX) project, which was a Japanese first entry experiment from orbit and successfully flied on February 4, 1994. Another is the Hypersonic Flight Experimet(HYFLEX) project, which is planned to be launched by J- I Rocket on February, 1996. These flight experimental resuts will give us much information about the aerothermodynamic environ-ment during reentry. But this information is not enough to design HOPE Orbiter. Because OREX and HYFLEX configurations are much different from HOPE; OREX is a capsule type Orbiter and HYFLEX has only fins on the body for lateral stability control, but HOPE is a winged Orbiter with tipfins. This difference means that the problem of local high heating rate caused by the nose bow-shock and leading edge-shock interference still remains. Because the basic configuration of HOPE is a double delta type, a shock interference heating will be an inevitable problem, especially in high temperature hypersonic flight regime, where nose bow-shock is close to the body because of the real gas effect.

To investigate the real gas effect, some high enthalpy shock tunnels were built. But They are not matured yet and they can not simulate completely the real condition. CFD technique, which is not also matured on high enthalpy flows, is required to supplememt the wind tunnel test data.

High enthalpy shock tunnel test was performed at HEG to investigate the real gas effect on heat transfer distribution along the sphere and on shock interference heating for a simple wing-body model, whose sweep-back angle on the starboad side is 55° and on the port side is 60° . The results of the heat transfer measurements are shown and the comparisons of CFD result on heat transfer distribution about the sphere model with experiment are made in this paper.

Test Facility

The HEG[1] is a so called free-piston driven shock tunnel capable of producing high enthalpy and high density test gas flow (figure 1). It is the largest free-piston shock tunnel in the world (60m total length). To create the high pressure of up to 100 MPa in the compression tube, a heavy piston (up to 800 kg and 500 mm in diameter) is used. The nozzle is the hypersonic contoured